Development 138, 5177-5188 (2011) doi:10.1242/dev.067868

A Trio-RhoA-Shroom3 pathway is required for apical constriction and epithelial invagination

Timothy F. Plageman, Jr[1,2], Bharesh K. Chauhan[1,2], Christine Yang[1,2], Fanny Jaudon[3], Xun Shang[4], Yi Zheng[4], Ming Lou[5], Anne Debant[3], Jeffrey D. Hildebrand[6] and Richard A. Lang[1,2,7,8,*]

SUMMARY

Epithelial invagination is a common feature of embryogenesis. An example of invagination morphogenesis occurs during development of the early eye when the lens placode forms the lens pit. This morphogenesis is accompanied by a columnar-to-conical cell shape change (apical constriction or AC) and is known to be dependent on the cytoskeletal protein Shroom3. Because Shroom3-induced AC can be Rock1/2 dependent, we hypothesized that during lens invagination, RhoA, Rock and a RhoA guanine nucleotide exchange factor (RhoA-GEF) would also be required. In this study, we show that Rock activity is required for lens pit invagination and that RhoA activity is required for Shroom3-induced AC. We demonstrate that RhoA, when activated and targeted apically, is sufficient to induce AC and that RhoA plays a key role in Shroom3 apical localization. Furthermore, we identify Trio as a RhoA-GEF required for Shroom3-dependent AC in MDCK cells and in the lens pit. Collectively, these data indicate that a Trio-RhoA-Shroom3 pathway is required for AC during lens pit invagination.

KEY WORDS: Apical constriction, Invagination, Rho GTPases, RhoGEF, Shroom, Mouse, Chick

INTRODUCTION

The development of complex structures during embryogenesis requires tightly controlled cell behaviors. For epithelial cell sheets undergoing morphogenesis, these behaviors include evagination and invagination to produce the folding that is characteristic of many structures. These epithelial movements can be generated through modulation of the cytoskeletal architecture of individual cells that, in aggregate, result in coordinated epithelial movements (Lecuit and Lenne, 2007).

Embryonic lens development serves as a useful model to study the mechanisms of epithelial bending (Chauhan et al., 2009; Plageman et al., 2010). Formation of the lens placode, a thickened region of head surface ectoderm located adjacent to the underlying optic vesicle, marks the first morphological sign of lens development. Shortly after lens placode development, the lens pit is produced through inward bending, or invagination, of the placode. This process occurs simultaneously with invagination of the underlying optic vesicle and is facilitated by the presence of filipodia and extracellular matrix that spans the space between the two epithelia (Chauhan et al., 2009; Huang et al., 2011).

Lens pit invagination is also accompanied by a coordinated cell shape change termed apical constriction (AC) in which epithelial cells adopt a wedge or conical shape (Hendrix and Zwaan, 1974; Plageman et al., 2010). The mechanism that drives AC involves activation of non-muscle myosin, which contracts the apical actin meshwork leading to reduction of the apical circumference (Sawyer et al., 2010). Shroom3, an actin-binding, cytoskeletal protein, is a principal regulator of AC during lens pit invagination (Plageman et al., 2010). Shroom3 was initially identified in a gene-trap screen as a critical factor required for mouse neural tube closure (Hildebrand and Soriano, 1999). When Shroom3 was depleted in the neural plate of *Xenopus* embryos, AC was prevented and the neural tube failed to close, as also observed in the mouse mutant (Haigo et al., 2003; Lee et al., 2007). Shroom3 drives AC by interacting directly with Rock1 and Rock2 (Rock1/2), serine/threonine kinases that function to activate non-muscle myosin and are themselves activated by the Rho family GTPase RhoA (Riento and Ridley, 2003; Nishimura and Takeichi, 2008). When disrupting the association between Shroom3 and Rock1/2 or chemically inhibiting Rock1/2 function, Shroom3 fails to induce AC, leading to neural tube closure defects (Wei et al., 2001; Hildebrand, 2005; Nishimura and Takeichi, 2008). Although Shroom3 is required for AC, it remains unclear whether Rock1/2 is involved during lens pit invagination or how Shroom3 influences Rock1/2 activity.

Guanine nucleotide exchange factors (GEFs) are a family of proteins that activate Rho-GTPases by catalyzing the conversion of the GDP-bound, inactive form into the GTP-bound, active form (Jaffe and Hall, 2005). GEF activity regulates embryonic development in *Drosophila* by affecting several cellular events including cytokinesis, migration and AC (Barrett et al., 1997; O'Keefe et al., 2001; Smallhorn et al., 2004; van Impel et al., 2009). By contrast, few vertebrate GEFs have established roles in embryogenesis. The GEF Trio is an exception and is required for skeletal muscle and neuronal development (O'Brien et al., 2000; Peng et al., 2010). Trio, and its homolog Kalirin, are unique in that

[1]The Visual Systems Group, Cincinnati Children's Hospital Medical Center, University of Cincinnati, Cincinnati, OH 45229, USA. [2]Division of Pediatric Ophthalmology, Cincinnati Children's Hospital Medical Center, University of Cincinnati, Cincinnati, OH 45229, USA. [3]Universités Montpellier 2 et 1, CRBM CNRS UMR 5237, 1919 Route de Mende 34293, Montpellier, CEDEX 5, France. [4]Experimental Hematology and Cancer Biology, Cincinnati Children's Hospital Medical Center, University of Cincinnati, Cincinnati, OH 45229, USA. [5]Department of Chemistry and Physics, Lamar University, Beaumont, TX 77710, USA. [6]Department of Biological Sciences, University of Pittsburgh, Pittsburgh, PA 15260, USA. [7]Developmental Biology, Children's Hospital Research Foundation, Cincinnati Children's Hospital Medical Center, University of Cincinnati, Cincinnati, OH 45229, USA. [8]Department of Ophthalmology, Cincinnati Children's Hospital Medical Center, University of Cincinnati, Cincinnati, OH 45229, USA.

*Author for correspondence (Richard.Lang@cchmc.org)

Accepted 27 September 2011

they have two distinct GEF domains: one that specifically activates Rac1 and RhoG (GEFD1) and another that activates only RhoA (GEFD2) (Debant et al., 1996; Alam et al., 1997). Much of the function of Trio and Kalirin during development has been attributed to the GEFD1 domain but the GEFD2 domain has not been analyzed in vertebrates (Newsome et al., 2000; Backer et al., 2007; Briancon-Marjollet et al., 2008).

As Shroom3-induced AC can be Rock1/2 dependent (Hildebrand, 2005; Nishimura and Takeichi, 2008), we hypothesized that during lens invagination, RhoA, Rock and a RhoA GEF would also be required. In this study, we show that Rock1/2 activity is required for lens pit invagination and that RhoA activity is required for Shroom3-induced AC. We demonstrate that RhoA, when activated and targeted apically, is sufficient to induce AC and that RhoA plays a key role in Shroom3 apical localization. Furthermore, we identify Trio as a RhoA-GEF required for Shroom3-dependent AC in MDCK cells and in the lens pit. Collectively, these data indicate that a Trio-RhoA-Shroom3 pathway is required for AC during lens pit invagination.

MATERIALS AND METHODS

Mouse maintenance and use

In accordance with institutional policies, mice were housed in a pathogen-free vivarium. Mouse embryos were isolated at specific gestational ages utilizing vaginal plug detection to define a gestational age of 0.5 days. Embryos were fixed in 4% paraformaldehyde and stored in PBS for further analysis.

Chick embryo culture/electroporation

Standard pathogen-free (SPF) fertilized chicken eggs (Charles River Laboratories) were incubated in a humid environment at 37.5°C for ~45 hours to obtain stage 11 embryos. Live embryo cultures were prepared and electroporated as previously described (Plageman et al., 2010). Experimental embryos were incubated with media containing 50 μm Y27632 for 5 or 16 hours. For whole-mount analysis of drug-treated embryos, a local dose of 50 μm Y27632 was administered on the left side adjacent to the lens placode using a pulled glass capillary and mouth pipette (Sigma, A5177); the right eye served as a negative control. Embryos were analyzed after 3.5 hours.

Antibody labeling

Cryosection immunofluorescence (IF) labeling was performed as described (Smith et al., 2005). The primary antibodies used were: anti-β-catenin (1:500, Santa Cruz, sc-7199), anti-ZO1 (1:500, Invitrogen, 61-7300), anti-Flag (1:500, Sigma, F1804), anti-V5 (1:500, Invitrogen, 46-0705), anti-E-cadherin (1:250, BD Biosciences, 610182), anti-phospho-myosin light chain (1:2500, Genetex, GTX22480), anti-β-crystallin (1:100) (Smith et al., 2009), anti-α-crystallin (1:1000) and anti-prox1 (1:1000, Millipore, AB5475). Alexa Fluor secondary antibodies were used at 1:1000 (Invitrogen, A10680, A-11012, A-11001, A-11019, A-21207). The Shroom3-specific rabbit polyclonal antibody (1:1000) was a generous gift from Jeff Hildebrand (Hildebrand, 2005). F-actin was visualized using Phalloidin staining (1:1000, Invitrogen, A12381, A12379). Nuclear visualization of cryosections was performed with Hoechst 33342 (1:1000, Sigma, B-2261). Whole embryo staining was performed in the same manner as for the cryosections.

In vitro binding assays

Sequences encoding amino acids 594-1060, containing both the Shroom3 SD2 and RhoA binding sites from human ROCK1 (Fujisawa et al., 1996; Nishimura and Takeichi, 2008; Bolinger et al., 2010), was cloned into pGex3X and expressed in BL21 *Escherichia coli*. Following isopropyl-β-D-thio-galactoside (IPTG) induction, cells were lysed by sonication in NETN (20 mM Tris pH 8.0, 100 mM NaCl, 1 mM EDTA, 0.5% NP-40, protease inhibitor cocktail) and purified using glutathione-sepharose. Sequences encoding mouse Shroom3 SD2, spanning amino acids 1731-1952, and constitutive active $RhoA^{L63}$ were cloned into pET151D/topo and pET28A, respectively, and expressed in BL21 *E. coli*. Following induction with IPTG, cells were lysed by sonication in lysis buffer (25 mM Tris pH 8.0, 500 mM NaCl, 10% glycerol, 5 mM imidazole, 5 mM β-mercaptoethanol) and His-tagged proteins purified using nickel affinity chromatography. Shroom3 SD2 and $RhoA^{L63}$ were eluted from the beads using 500 mM imidizol, 150 mM NaCl, 5%, glycerol. For in vitro binding, GST-Rock (5-7 mg) bound to beads was mixed with 10 mg of RhoA or Shroom3 SD2 in a total volume of 50 ml and incubated for 1 hour at room temperature with constant rocking. Supernatant was removed and the beads washed five times in NETN. Beads were resuspended in 30 ml of sample buffer and supernatant and bead fractions resolved by SDS-PAGE and proteins detected by Coomassie Blue staining.

Immunofluorescence quantification

The IF intensity along the apical/basal axis was determined from cryosections (10 μm) fluorescently labeled with antibodies specific for phospho-myosin regulatory light chain (pMRLC) and Shroom3 using Image J v1.33. The average pixel intensity was quantified from ≥17 cells of four to six lens pits following normalization to the average IF intensity of each image and normalization to cell height.

Morphometric analysis

The average cell shape and apical area was quantified as previously described (Plageman et al., 2010). In brief, all of the cell outlines from IF-labeled cryosections of six mouse lens pits were traced and normalized to cell height, and the cell width was measured at seven equally spaced points along the apical-basal axis. Approximately 50-100 transgenic chicken lens pit cells from a total of five to ten embryos were quantified in the same manner. The average apical area of lens placodal and transgenic MDCK cells was quantified from tracing the apical junctional area and analyzing the outlines in Image J v1.33. Transgenic cells used for quantification were pre-screened by analyzing their nuclei (Hoeschst staining) to avoid those undergoing cytokinesis or apoptosis as these processes can influence cell shape. For the transgenic cells used in the quantitative analysis, a reduction in AC was assumed for cells with a decreased apical area. For MDCK cells, several cells for each condition were analyzed from at least two to seven independent experiments. The exact number of cell outlines is depicted in each figure.

Lens pit shape analysis

Coordinates were extracted from curves representing the basal surface of the lens pit using Matlab 7.1 (The MathWorks, MA, USA). The functional form of each curve was calculated by fitting and interpolating the coordinates. Curves were then averaged and a graph was generated by Mathematica 7.0 (Wolfram Research, IL, USA).

Statistics

Statistical analyses for most data sets were performed using the statistical software SPSS 13. The means were analyzed using one-way ANOVA with the following post-hoc tests: Dunnett's (Fig. 2A,C,F), Tukey's (Fig. 4D), Bonferonni (Fig. 5B). Student's *t*-test was applied to the data shown in Fig. 1P. Statistical significance was assumed when $P<0.05$. For analysis of the immunofluorescence data shown in Fig. 3G,H,I and Fig. 6E, a regression model was analyzed that corresponded to a two-way analysis of variance. In addition, group variances were allowed to differ in order to increase the precision of group means and the detection of a significant difference between means. The fit of regression models improved after pixel intensity levels were $\log_e$ transformed, as determined by the Akaike Information Criteria (Akaike, 1974); therefore geometric means and confidence intervals were calculated, and statistical significance was based on the results of $\log_e$-transformed expression data. The Holm-Sidak method of adjusting for false discovery rates was applied to determine adjusted significance levels for detecting differences between group means ($\alpha=0.05$). The analyses were performed using SAS for Windows, Version 9.2.

DNA constructs and transfection

MDCK cells were transiently transfected with 1 μg of the indicated plasmid when reaching ~30% confluency using a lipofectamine reagent (TransIT-293, Mirus) according to the manufacturer's instructions.

Transfected MDCK cell cultures were incubated for an additional 48 hours and, when indicated, were treated with the following chemicals: Y27632 (20 μg/ml CalBiochem), blebbistatin (50 μg/ml, CalBiochem), G04 (50 μM) and Y16 (50 μM) for 90 minutes prior to fixation and staining. To generate the apically and basolaterally targeted RhoA, the expression vectors Mieg3-RhoA^{wt}, Mieg3-RhoA^{N19} and Mieg3-RhoA^{L63} were used as DNA templates in a PCR reaction with the primers 5′-TAGGATCC-ATGGCTGCCATCCGGAAGAAA-3′ and 5′-CAAGACAAGGCA-CCCAGATTT-3′, and the amplified sequence was ligated into the pcDNA3.1/V5-His TA vector (Invitrogen, K4800-01). To generate the VSV-G fusion constructs, PCR was performed using the pCMV-VSV-G plasmid (Addgene, 8454) (Stewart et al., 2003) as template DNA and the primers 5′-TAGGATCCCACCATGAAGTGCCTTTTGTACTTA-3′ and 5′-ATGGATCCCTTTCCAAGTCGGTTCATCTC-3′ (Fisher) and the amplified sequence was ligated into the PCR II vector (Invitrogen, K2050-01). The plasmid was then digested with *Bam*H1 and cloned into the *Bam*H1 site of the pcDNA3.1-RhoA vectors immediately 5′ of the RhoA cds. The *Fcgr2b* fusion genes were made in a similar manner but using the PCR primers 5′-TAGAATTCCACCATGGGAATCCTGCCGTTCCTA-3′ and 5′-ATGAATTCAATGTGGTTCTGGTAATCAT-3′, with E10.5 mouse embryo cDNA as template, and the *Eco*R1 restriction enzyme for cloning. The Tripα primary sequence was generated through amplifying the partially complementary primers 5′-ACCATGGCGTCTGAAGGTGC-TGACGGTGCTATCTGTGGCTACAACTTAGCGACGCTAGTCATGTT-AGGACCTAGCGAAC-3′ and 5′-CATCAATTCATAGATATCAGAAGA-ACATGGCTCGCACAGTGGGCAGAATACGCGTTCGCTAGGTCCTA-ACATGACTAGCG-3′ (Fisher), which code for the Tripα amino acids and a Kozak sequence. Once amplified, the PCR product was ligated into the pcDNA3.1/V5-His TA vector (Invitrogen, K4800-01). The vectors expressing Trio, shTrio (Charrasse et al., 2007), Trio^{wt}-GFP and Trio$^{Q1368A/L1376E}$-GFP (Estrach et al., 2002), Trio^{L2051E}-GFP (Bellanger et al., 2003) and Shroom3-Flag (Plageman et al., 2010) have been described previously. A Kalirin-deficient cell line was generated by stable expression via puromycin selection of a Kalirin shRNA lenti-viral vector (TRCN0000048208, Sigma).

RNA isolation, RT-PCR and in situ hybridization

RNA was isolated from microdissected embryonic chick eyes from ~12 embryos at the indicated stages and MDCK cells using Trizol (Invitrogen)/chloroform extraction. RNA was isolated in the same manner from mouse lens cells after they were flow-sorted for GFP. GFP+ lens cells were isolated from embryonic day (E) 10.5, *Le-cre* (Ashery-Padan et al., 2000) hemizygous mice. Microdissected eyes were dissociated (0.05% trypsin for 5 minutes; quenched with 10% then 2% FBS for 5 minutes each; triturated 30 times with centrifugation between incubations) and then sorted using standard methods. Sorting generated a small population (1% of the total) of GFP+ cells. After RNA isolation, RT-PCR was performed by generating coda using the SuperScript First-Strand Synthesis kit (Invitrogen, 11904-018) and the following primers: chicken Trio 5′-AGGAGAGACCATCGTGCTTAGGTG-3′, 5′-ACTTAGTGGCTACT-GCTCGCTTG-3′; mouse Trio 5′-AGGGGAGACCGTTGTTTTTA-GATG-3′, 5′-ACTTTGTGGCCACTGCTCGTT-3′; chicken Kalirin 5′-AGGCAATTGCACCATTTCTGGCTA-3′, 5′-GAATTTTACAGCCA-CGTCTTCC-3′; mouse Kalirin 5′-GGATCCCAGTGCCTCGAGTGA-3′, 5′-GGCTGTAGCCAGGGATGCTGC-3′; mouse Foxe3 5′-TACT-CATACATCGCGCTCATTG-3′, 5′-GGAAGCTACCGTTGTCGAACAT-3′; and mouse L7 5′-GAAGCTCATCTATGAGAAGGC-3′ and 5′-AAGACGAAGGAGCTGCAGAAC-3′. The mouse primers were used for MDCK cell RT-PCR. The δ-crystallin in situ hybridization probe was generated by performing PCR on embryonic stage 14 cDNA using the primers 5′-GAGGAATCATCTAAGGGAT-3′ and 5′-TCCTTGCT-GAAGGTGCTTGG-3′, and ligating the amplified sequence into the PCRII vector using the TA cloning kit (Invitrogen, K2060-01). The plasmid was linearized with *Xho*I (NEB) and the probe amplified with Sp6 polymerase (Promega), and digoxigenin (DIG)-labeled nucleotides (Roche). The hybridization protocol used was as described previously (Toresson et al., 1999).

RESULTS

Rho kinase activity is required for lens pit invagination and apical constriction

During neural tube closure, the interaction between Shroom3 and Rock1/2 is necessary for AC and subsequent morphogenesis (Nishimura and Takeichi, 2008). Lens pit invagination involves Shroom3-induced apical constriction but it is unclear whether Rho-kinase activity is also required. To test this, chicken embryos were cultured in the presence of the Rho-kinase inhibitor Y27632 (Fig. 1). After 5 hours in culture, the lens pit normally initiates invagination and expresses the lens differentiation marker δ-crystallin (Fig. 1B). In the presence of Y27632, the placode initiated δ-crystallin expression but did not invaginate (Fig. 1C). The lack of δ-crystallin expression in control embryos at a comparable placodal stage (Fig. 1A) demonstrates that failure to invaginate is not due to developmental delay. To assess this further, embryos were cultured for 16 hours in the presence of the Rock-inhibitor (Fig. 1D-O). Almost half (15/31) of the Y27632-treated embryos, compared with 3/39 of control embryos, lacked lens pit invagination and exhibited a flattened placodal structure. Although the lens pit failed to form, several lens differentiation markers were strongly expressed in the placode (Fig. 1D-O) indicating that morphogenesis failed without an alteration in cell fate acquisition. To determine whether the lack of invagination could be due to an inhibition of AC, the apical area of lens placodal cells was measured. Compared with the control, the average apical area of placodal cells from Y27632-treated embryos after 3.5 hours in culture was significantly larger (Fig. 1P-T). Because a reduction in apical area is normally indicative of AC in the lens placode (see the wedge-shaped cells in Fig. 5), it is assumed that the reduced area observed in Y27632-treated embryos is due to a failure of Rho-kinase dependent AC.

RhoA activity is required for Shroom3-induced apical constriction

MDCK cells are polarized epithelial cells that can be induced to apically constrict (Hildebrand, 2005). To determine whether RhoA is sufficient to cause AC, we transiently transfected MDCK cells with RhoA-containing constructs and measured the apical area of individual cells (Fig. 2A,B). As we found that wild-type RhoA and constitutively active RhoA (RhoA^{L63}) were insufficient to induce AC (Fig. 2B), we hypothesized that apical localization was necessary. Interestingly, we found that when either RhoA or RhoA^{L63} were fused to VSVG (hereafter Ap-RhoA and Ap-RhoA^{L63}), a protein normally localized basolaterally, the fusion proteins efficiently localized to the apical membrane (Fig. 2B). We then used these constructs to determine whether apical localization of RhoA was sufficient to induce AC and found that AC occurred in Ap-RhoA^{L63}-expressing cells but not Ap-RhoA cells (Fig. 2A,B). Not surprisingly, the induction of AC by Ap-RhoA^{L63} was found to be dependent on Rho-kinase and myosin II function as the inhibitors Y27632 and blebbistatin prevented the cells from apically constricting (Fig. 2A,B). AC is not inhibited when Ap-RhoA^{L63} transfected cells were treated with a chemical inhibitor of RhoA (G04) designed to block access of RhoA to GEFs (X.S. and Y.Z., unpublished). These data indicate that apically localized, active RhoA is sufficient for AC and that activation of RhoA without localization is inadequate. Activating apically targeted wild-type RhoA by co-transfecting the RhoA GEF Trio also caused AC (Fig. 2A,B) suggesting that, once apically localized, RhoA is capable of inducing AC upon stimulation by a RhoGEF.

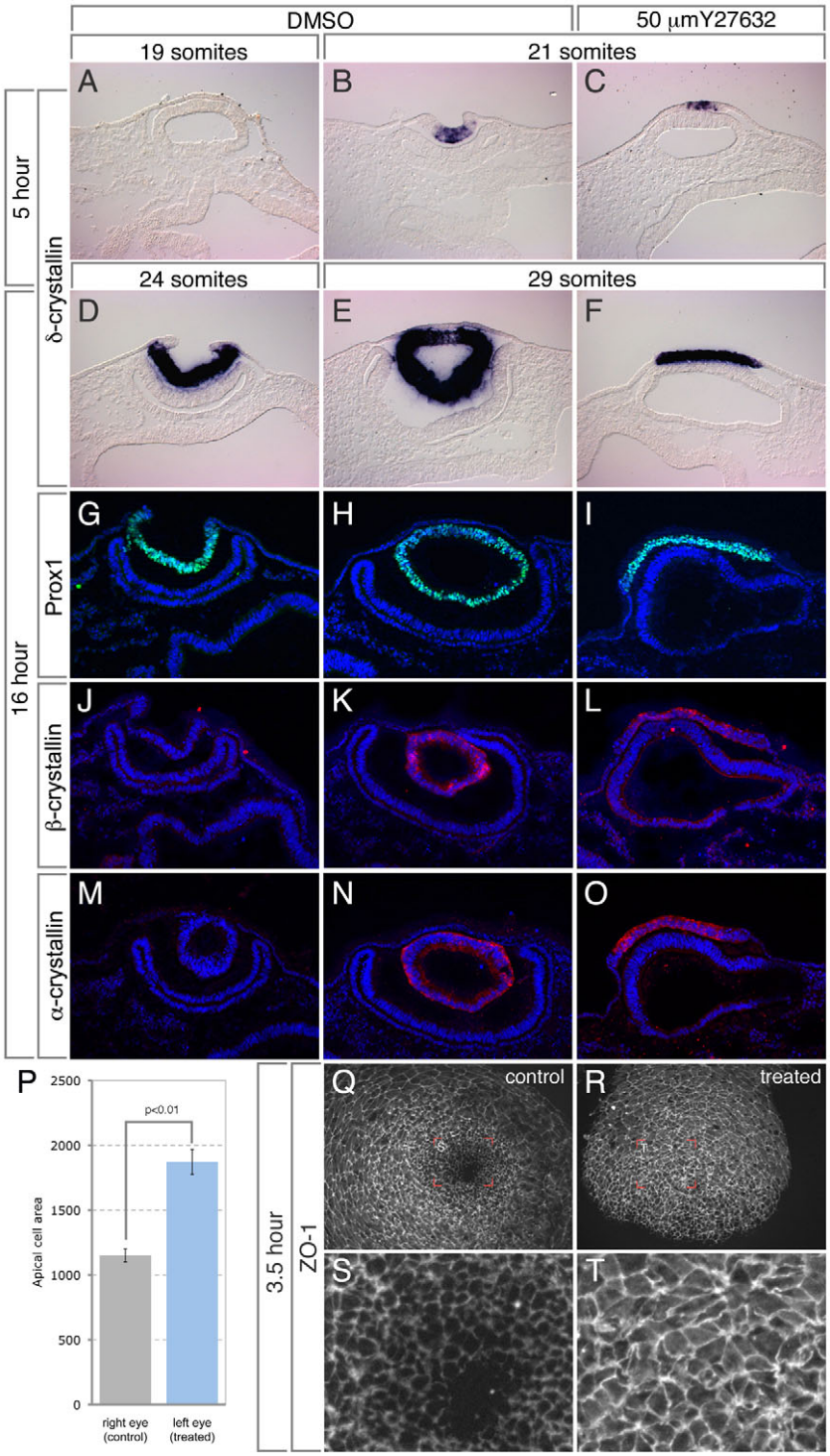

Fig. 1. Rock1/2 activity is required for lens pit invagination and apical constriction. (**A-F**) In situ hybridization of cryosectioned chicken embryos cultured in the presence of DMSO (A,B,D,E), or 50 mM Y27632 (C,F) for the indicated time, using a probe specific for δ-crystallin, an early lens differentiation marker. Embryos were age matched according to somite number. (**G-O**) Cryosections of chicken embryos cultured for 16 hours were immunofluorescently labeled (green or red) with the indicated lens differentiation markers. Hoechst staining was performed simultaneously to visualize the nuclei (blue). (**P-T**) A local dose of Y27632 was administered to the left eye of stage 13 chick embryos and cultured for 3.5 hours. The embryos were immunofluorescently labeled for ZO1 to mark the apical junctions of the right control eye (Q,S) or the Y27632-treated eye (R,T). The average apical area of cells from each eye was quantified and is depicted in the graph (P). Error bars represent s.e.

Previous work has shown that Shroom3 induces AC in MDCK cells and that inhibition of Rho-kinase and non-muscle myosin activity obstructs the process (Hildebrand, 2005). Although RhoA is an activator of Rock1/2, a positive role for RhoA during Shroom3-induced AC has not been demonstrated. Co-transfection of Shroom3 with a dominant-negative form of RhoA (RhoAN19) or treatment of Shroom3-positive cells with the RhoA chemical inhibitor G04, both prevent AC (Fig. 2C,D). Unlike G04, which inhibits RhoA by preventing association with all GEFs, Y16, a chemical inhibitor that blocks only RGS domain-containing GEFs (X.S. and Y.Z., unpublished) does not block Shroom3-induced AC. Together, these data indicate that Shroom3-induced AC requires active RhoA, and suggests that the activation is achieved by a non-RGS domain-containing GEF.

Results from the genetic and cell culture assays suggest that RhoA, Shroom3 and Rock work together to regulate apical constriction. To validate these observations biochemically, we used an in vitro binding and pull-down assay to determine whether these proteins can form a complex. A GST-fusion protein of human ROCK1 encompassing amino acids 594-1060 and containing both

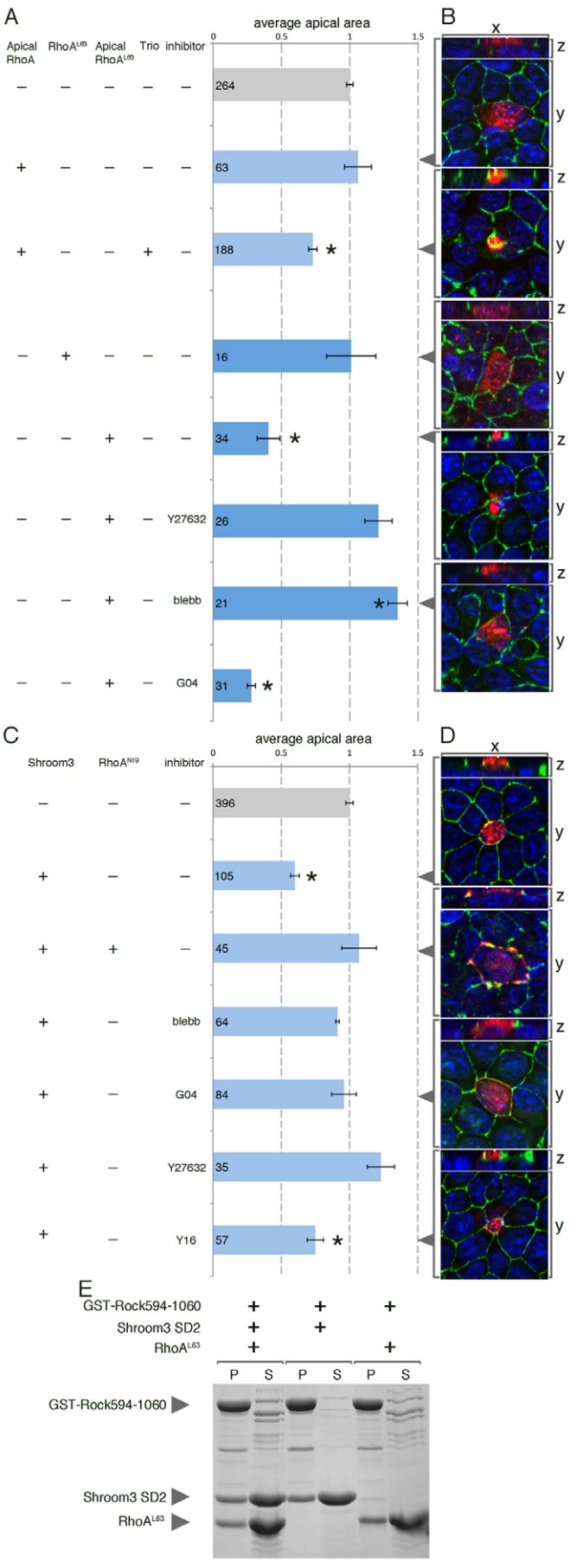

Fig. 2. RhoA activity is required for Shroom3 induced apical constriction. (**A-D**) MDCK cells were transfected with the indicated expression plasmid and subsequently treated with the specified chemical inhibitor. Immunofluorescent labeling of ZO1 (green) was used to visualize the apical junctions, and for the epitope tags (red), to visualize transfected RhoA (B) or Shroom3 (D). Apical views of cells are visualized in the *xy* plane and the apical-basal axis is visualized in the *xz* plane. The average apical area for cells was calculated for each condition and is displayed in the bar graphs (A,C). Error bars represent s.e.m. **P*<0.05. (**E**) The amino acids 594-1060 of Rock1 fused to GST, constitutively active RhoA ($RhoA^{L63}$) and the Rho-kinase binding domain of Shroom3 (SD2) were bacterially expressed and used in a pull-down assay. Coomasie Blue staining of an SDS-PAGE gel reveals protein that was resolved from the pellet fraction (P), which indicates binding to GST-Rock1, or from the supernatant (S).

the Shroom3 and the RhoA binding domains was expressed and purified from bacteria. GST-ROCK immobilized on beads was mixed with equal amounts of soluble Shroom3 SD2 and constitutively active RhoA ($RhoA^{L63}$) and the resultant protein complexes purified, resolved by SDS-PAGE, and detected by Coomassie Blue staining. GST-ROCK successfully pulled-down both $RhoA^{L63}$ and the Shroom3 SD2 in roughly equal stoichiometry (Fig. 2E). Importantly, equal amounts of RhoA and SD2 were precipitated by GST-ROCK regardless of whether they were added alone or in combination, suggesting that RhoA and Shroom3 can bind to Rock simultaneously and do not compete for binding.

Apical RhoA activity is necessary and sufficient for Shroom3 apical localization

Similar to RhoA-induced AC, Shroom3-induced AC is dependent on apical localization (Hildebrand, 2005; Bolinger et al., 2010), but the mechanism underlying apical recruitment is unknown. Because RhoA is known to regulate cell polarity (Fukata et al., 2003), we determined whether RhoA regulated Shroom3 localization (Fig. 3). As might be anticipated, MDCK cells expressing Ap-$RhoA^{L63}$ had a normal distribution of Shroom3 in the apical junctions (Fig. 3A). By contrast, when $RhoA^{L63}$ was basolaterally targeted in MDCK cells, accomplished by fusing $RhoA^{L63}$ with Fcgr2b sequences (hereafter Bl-$RhoA^{L63}$), Shroom3 was localized to the basal end of the cell in junction-like structures (Fig. 3B). Bl-$RhoA^{L63}$ also induced basal constriction, as the basal area was consistently smaller than the apical area (Fig. 3B,C). Because the Shroom3-expressing basal junction structures in Bl-$RhoA^{L63}$-expressing cells resembled mislocalized tight junctions, immunolabeling of ZO1, a tight-junction adaptor protein, was performed. ZO1 was notably absent from the apex of Bl-$RhoA^{L63}$-expressing cells (Fig. 3C); however, strong ZO1 localization was observed basolaterally (Fig. 3C,D), consistent with the idea that tight junctions are mislocalized in these cells. These data demonstrate that the localization of activated RhoA is sufficient to direct apical or basal recruitment of Shroom3 and apical or basal constriction.

To determine whether RhoA directs Shroom3 localization in the lens pit during invagination, *RhoA* mutant mouse embryos were analyzed at E10.5. The conditional $RhoA^{fl}$ allele (Chauhan et al., 2011) was recombined in the lens pit using the *Le-cre* transgenic line (Ashery-Padan et al., 2000), which causes decreased AC and reduced lens pit curvature (Chauhan et al., 2011) (Fig. 6C).

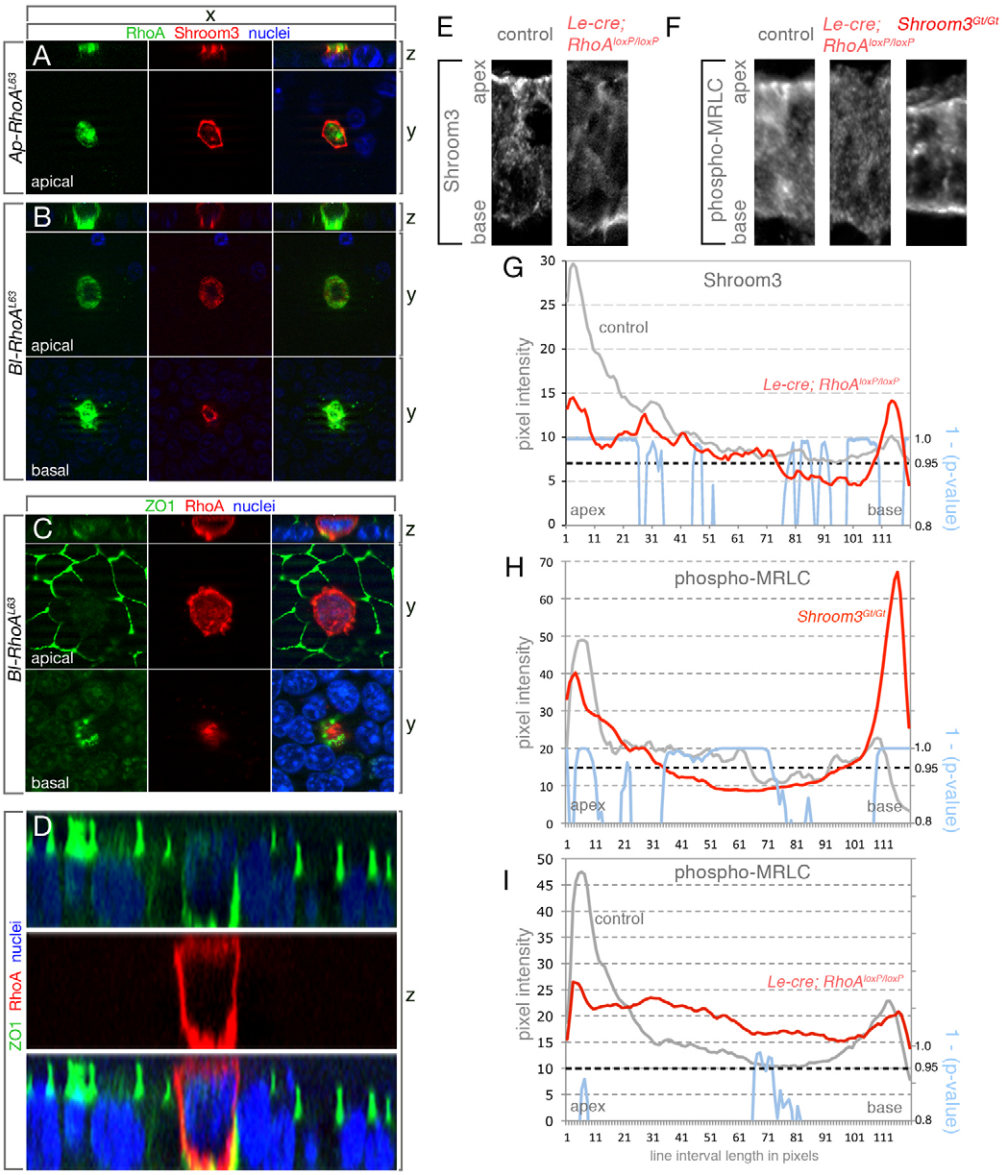

Fig. 3. RhoA activity is necessary and sufficient for Shroom3 apical localization. (**A**,**B**) Immunofluorescent labeling of MDCK cells co-expressing exogenous Shroom3 (red) and regionally targeted versions of constitutively active RhoA (green). Nuclei are in blue. The *xz* plane allows visualization of the apical-basal axis and the *xy* plane a view of the apex or base. The *xz* view shows that VSVG-RhoA^{L63} (Ap-RhoA^{L63}) is targeted apically (A) whereas Fcgr2b-RhoA^{L63} (Bl-RhoA^{L63}) targets basolaterally (B). (**C**) Immunofluorescent labeling for ZO1 (green) of an MDCK cell expressing Bl-RhoA^{L63} (red). Nuclei are in blue. (**D**) *xz* plane of a field of MDCK cells labeled for ZO1 (green) and nuclei (blue) in which one is expressing Bl-RhoA^{L63} (red). In this cell, ZO1 labeling is adjacent to the adhesion substrate. (**E**,**F**) Immunofluorescent labeling of Shroom3 (E) or phospho-MRLC (F) in wild-type or mutant E10.5 lens pit cryosections. (**G-I**) The average pixel intensity following immunolabeling with Shroom3 (G) or phospho-MRLC (H-I) specific antibodies was quantified over apical-basal line intervals for control (gray) or mutant (red) genotypes. The means are calculated from ≥17 cells from at least four different lens pits. Statistically significant differences were evaluated by calculating *P*-values (see Materials and methods) for each pixel along the apical-basal axis. The blue line indicates the trend of statistical *P*-values subtracted from 1 and values greater than 0.95 ($P<0.05$) indicate regions in which a statistically significant difference in signal intensity is found.

Conditional RhoA mutation also caused a dramatic reduction of apical localization of Shroom3 and an increased concentration of Shroom3 at the cell base (Fig. 3E,G). The phenotype of reduced AC in the conditional *RhoA* mutant (Chauhan et al., 2011) was similar to that observed in *Shroom3*$^{Gt/Gt}$ mutants (Plageman et al., 2010). Together, these data demonstrate that Shroom3 apical localization is dependent on RhoA and suggest that the RhoA phenotype is, at least in part, due to mislocalization of Shroom3.

During AC, phosphorylation of non-muscle myosin regulatory light chain (MRLC) occurs downstream of the RhoA-Rock pathway and activates its contractile function. Therefore, the presence of activated, phosphorylated MRLC serves as a useful indicator of RhoA-dependent AC. We assessed phospho-MRLC levels and localization in *RhoA* and *Shroom3* mutant embryos at E10.5, and observed that both exhibit a reduction in apical phospho-MRLC (Fig. 3F,H,I). Although the *RhoA* mutant on average displayed a large reduction in apical phospho-MRLC (Fig. 3I, red profile), statistical significance was not quite reached. The *Shroom3* mutant, however, did have a significantly reduced level of apical phospho-MRLC (Fig. 3H, red profile). A significant increase in basal phospho-MRLC was also observed in *Shroom3* mutants (Fig. 3H, green profile), consistent with the previously observed increase in basal non-muscle myosin (Hildebrand, 2005; Plageman et al., 2010). From these data, we conclude that Shroom3-induced AC depends on RhoA both for stimulating the contractile actin network through the activation of non-muscle myosin and for apically positioning Shroom3.

The RhoA guanine exchange factor Trio is required for Shroom3-induced AC

Although Shroom3 function depends on RhoA, it remained unclear how RhoA was activated. Because Shroom3 does not contain a DH/PH domain, the dual motif characterizing most known GEFs, it was unlikely to fulfill this requirement. In order to identify RhoA-GEFs expressed in the lens placode, RT-PCR analysis was performed on RNA isolated from MDCK cells (Fig. 4A), dissected embryonic chicken eyes (Fig. 4B), and mouse lens progenitors (Fig. 4C). Mouse lens progenitors were defined according to the

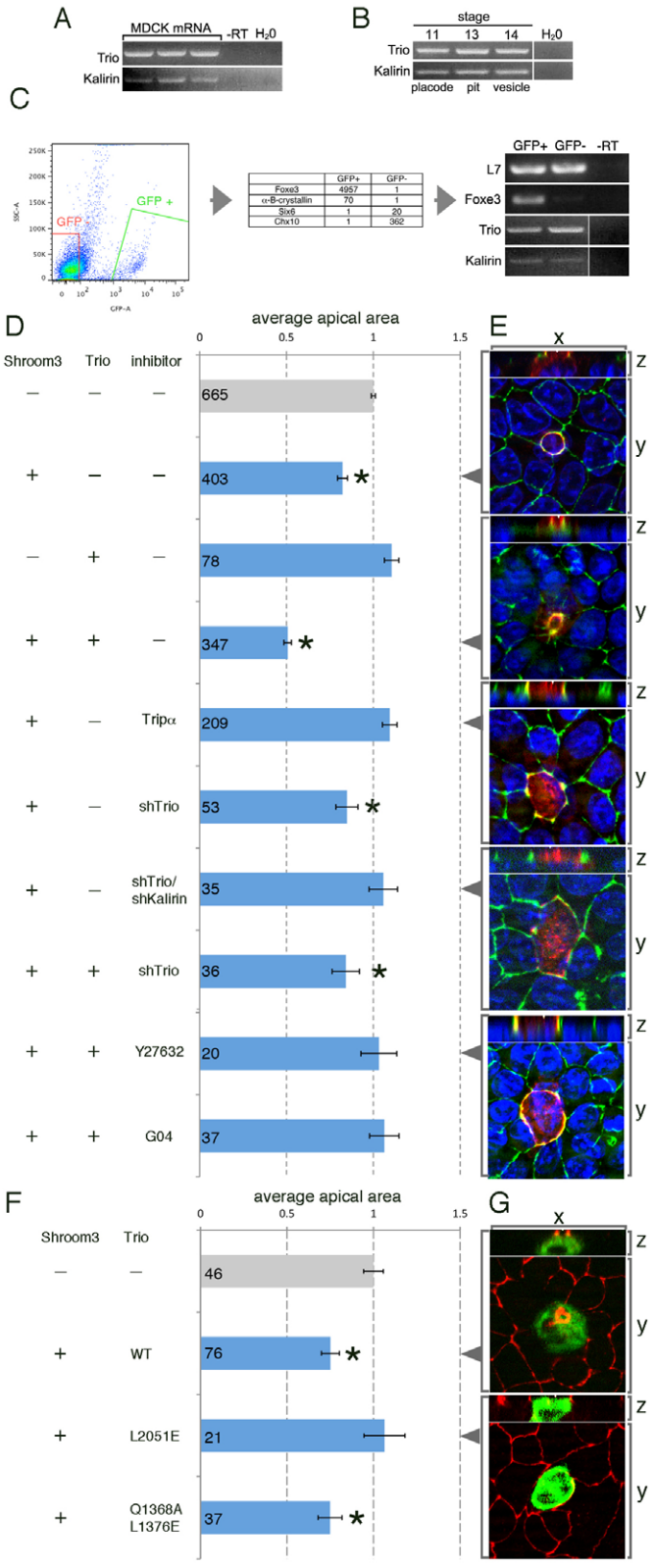

Fig. 4. Inhibition of the Trio RhoA-GEF domain prevents Shroom3 induced AC. (**A**,**B**) RT-PCR performed on RNA isolated from MDCK cells (A) or chicken embryo eyes from the indicated stages (B) reveals the presence of both *Trio* and kalirin mRNA. (**C**) Lens pit cells from the eye region of E10.5 transgenic mouse embryos expressing GFP (the *Le-cre* line) were isolated by flow cytometry. Scatter plot depicts the cell populations isolated. qPCR for lens and retina marker genes was performed on RNA from the GFP+ and GFP– cell populations. The fold expression difference is listed in the table. Both *Trio* and kalirin are expressed in the GFP+ and GFP– cell populations. –RT, without reverse transcriptase. (**D-G**) MDCK cells were transfected with the indicated plasmid(s). Where indicated, they were treated with Y27632 or G04. Immunofluorescent labeling of Shroom3-Flag (red, E) or Trio-GFP (green, G) was used to identify transfected cells. ZO1 labeling (green in E, red in G) allowed visualization and quantification of the apical area. Error bars represent s.e.m. and the asterisks identify experimental groups significantly different from the control ($P<0.05$). The number of cells analyzed for each experimental group is listed at the base of each bar in the histogram.

GFP expression of the *Le-cre* transgene that is dependent on Pax6 transcriptional control elements for expression (Ashery-Padan et al., 2000). Flow sorting of GFP+ lens progenitors from the dissected eyes of Le-cre embryos at E9.5 was validated by performing qPCR for expression of transcripts that were markers for either lens (FoxE3, αB-crystallin) or retina [Six6, Vsx2 (Chx10)]. This showed that GFP+ cells have dramatic fold increases in lens marker expression whereas the GFP– cells showed large fold increases in expression of retinal markers (Fig. 4C).

The closely related GEFs Trio and Kalirin were both detected in MDCK cells, in the developing chicken eye and in mouse lens progenitors (Fig. 4A-C). We then tested whether Trio could influence Shroom3-induced AC by expressing it in MDCK cells. This showed that Trio does not induce AC alone; however, when co-expressed with Shroom3, an enhanced effect on AC was observed and the apical cell area in cells expressing both was significantly smaller than with Shroom3 alone (Fig. 4D,E). The effect was abrogated by the addition of the Rho-kinase inhibitor Y27632, suggesting that Trio influences AC by activating the RhoA-Rock1/2 pathway (Fig. 4D,E). We also observed that Trio induces AC when co-expressed with apically targeted but otherwise wild-type RhoA, which by itself cannot cause AC (Fig. 2A). These data suggest that Trio influences AC by activating RhoA.

To ascertain whether Trio is required for Shroom3-induced AC, we depleted Trio via expression of a short-hairpin (sh) RNA. We found that AC mediated by Shroom3 is unaffected by shTrio expression (Fig. 4D) and deduced that compensation of Trio function might be occurring through Kalirin (Fig. 4A). The absence of a response in this assay is not likely to be due to ineffectiveness of the shRNA as the enhanced effect on AC mediated by Trio and Shroom3 was abolished with the addition of shTrio (Fig. 4D). To test whether Kalirin might be compensating for the lack of Trio, Kalirin was also depleted in MDCK cells. When both Trio and Kalirin were depleted, Shroom3 could not induce AC in MDCK cells. In order to inhibit Trio function in a different way, we used the polypeptide inhibitor Tripα. This was isolated from a screen designed to identify inhibitors specific for the RhoA activation domain (GEFD2) of Trio that did not affect the Rac1/RhoG activation domain (GEFD1) (Schmidt et al., 2002). When co-expressed with Shroom3, Tripα prevented AC in MDCK cells (Fig. 4D,E). The

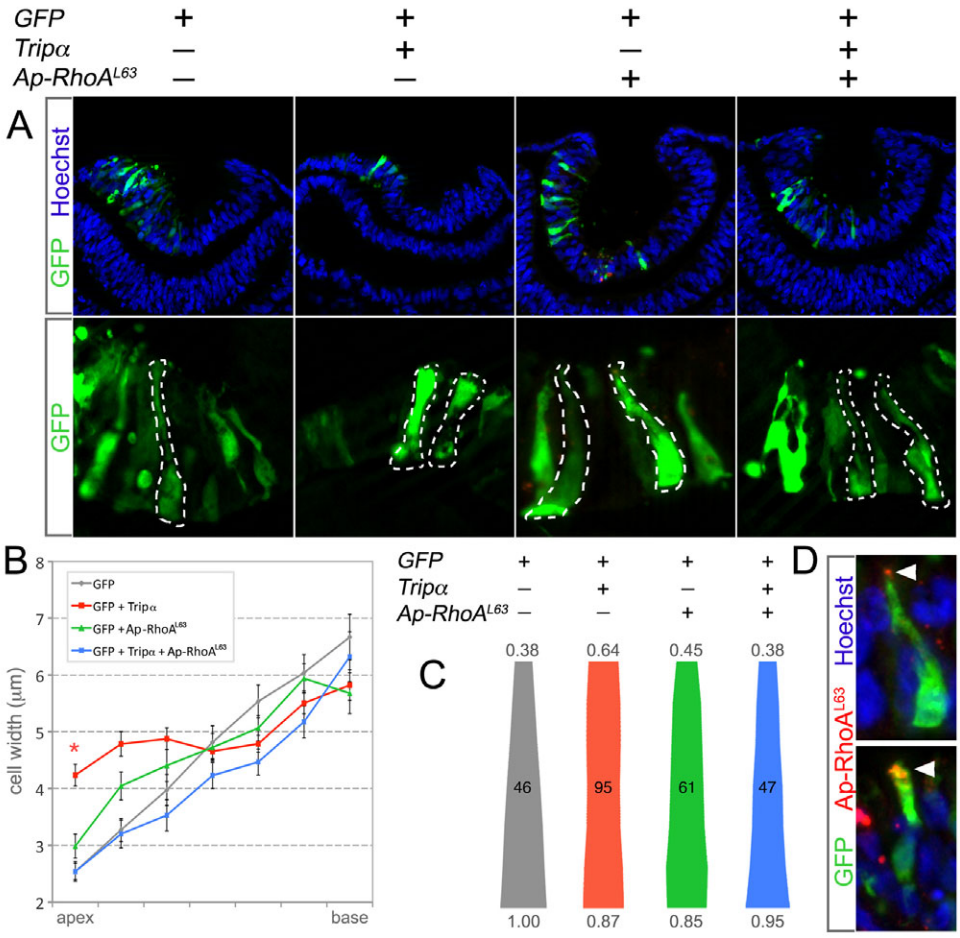

Fig. 5. Trio activation of RhoA is required for apical constriction during lens pit invagination. (**A**) Stage 11 chicken embryos were electroporated in ovo with the indicated plasmid(s) and allowed to develop until the lens pits began to invaginate. Transgenic embryos were cryosectioned and the outline of GFP-positive cells was determined (dashed lines). (**B**) The average apical width along the apical basal axis of transgenic cells from each experimental group is depicted. Error bars represent s.e.m. and the asterisk identifies significant differences from the control ($P<0.05$). (**C**) The average cell shape from each experimental group is depicted. The number value above or below each shape is the fold difference between the average basal width of control cells and the apical or basal widths, respectively, of the transgenic cells. The number of cells analyzed for each group is indicated in the middle of each outline. (**D**) Electroporated chicken lens pit cells labeled for GFP (green), nuclei (blue) and epitope tagged Ap-RhoA^{L63} (red). The arrowheads indicate the apical localization of Ap-RhoA^{L63}.

activity of the GEFD1 and GEFD2 domains can also be abrogated through previously defined mutations (Estrach et al., 2002; Bellanger et al., 2003). Shroom3-induced AC was inhibited when Shroom3 was co-expressed with Trio mutated in the GEFD2 (L2051E) but not the GEFD1 (Q1368A/L1376E) domain (Fig. 4F,G). Together, these data indicate that Shroom3-induced apical constriction in MDCK cells requires RhoA activation mediated by Trio.

These findings suggest that Trio might be required for Shroom3-induced AC in the lens pit. To investigate this, the Trio inhibitor Tripα was expressed in the prospective lens of chicken embryos via electroporation (Fig. 5). Co-expression of GFP indicated cell boundaries and allowed the quantification of individual cell shapes (Fig. 5A-C). This showed that control cells exhibited AC, whereas Tripα-positive cells had a significantly wider apex and a more columnar shape (Fig. 5B,C). We hypothesized that AC was reduced in Tripα-positive cells because activation of RhoA did not occur. To test this, we co-expressed Tripα with Ap-RhoA^{L63}, the apically targeted, activated mutant (Fig. 4A). Detection of Ap-RhoA^{L63} in chick lens pit cells via the epitope tag (Fig. 5D) confirmed that it was apically targeted. Furthermore, AC was completely restored in cells that expressed both Tripα and Ap-RhoA^{L63} (Fig. 5A-C). The apical width of Tripα- and Ap-RhoA^{L63}-expressing cells was not significantly different from control cells and the overall cell shape was very similar (Fig. 5A-C). These data suggest that Trio is required for RhoA activation to enable AC of cells within the lens pit during invagination.

To assess the requirement for Trio during lens pit invagination in the mouse, we analyzed lens development in the Trio mutant (O'Brien et al., 2000) using E10.5 cryosections (Fig. 6A,B). We first performed a quantitative assessment of E10.5 lens pit shape in control and *Trio*$^{-/-}$ mice (Fig. 6C, gray and red traces) and compared this with the lens pit shape of Le-cre; RhoA conditional mutants (Fig. 6C, blue trace). This revealed that the average shape of Trio mutant lens pits is shallower than control animals. Furthermore, the comparison of *Trio* and *RhoA* mutant lens pit shapes showed that they are very similar (Fig. 5C). This was consistent with the hypothesis that Trio activates RhoA during lens pit invagination. As a further test of this hypothesis, we performed labeling for phospho-MRLC as this is indicative of ROCK1/2 activity (Amano et al., 1996; Kimura et al., 1996; Totsukawa et al., 2000). This analysis showed that apical phospho-MRLC labeling is significantly reduced in the lens pit of *Trio*$^{-/-}$ embryos (Fig. 6D,E) indicating that the contractile actin-myosin network required for AC is not fully activated. We have also shown that the *Le-cre; RhoA*$^{fl/fl}$ conditional mutant has a reduced level of apical labeling for phospho-MRLC (Chauhan et al., 2011). Shape quantification of lens pit cells from *Trio*$^{-/-}$ embryos revealed that the apical width is significantly greater (1.3-fold) than in the wild type (Fig. 6F), consistent with the loss of activated apical myosin. The significant difference in cell shape argues that the lens pit phenotype in the Trio mutants not due to a general delay in development. Collectively, these data demonstrate a requirement for Trio during lens pit invagination and suggest that it initiates AC through the activation of RhoA.

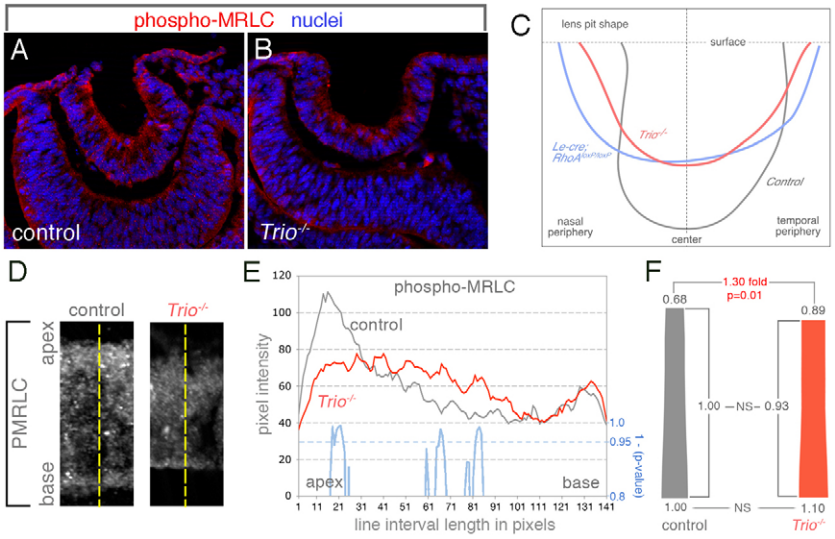

Fig. 6. Trio regulates apical constriction during mouse lens pit invagination. (**A**,**B**) Wild-type (A) or Trio-deficient (B) cryosectioned E10.5 mouse embryos were labeled for, phospho-myosin (red) and nuclei (blue). (**C**) Lines describing the apical surface curvature of lens pits from embryos of the indicated genotypes. The lines represent average curvature of lens pits from five embryos, compiled using coordinate geometry. (**D**) Examples of phospho-MRLC labeling of cryosectioned lens pits from control and Trio-deficient mouse embryos. The yellow lines depict the axes of immunofluorescent quantification. (**E**) The average pixel intensity along apical-basal line intervals (depicted in D) in lens pit cells from control (gray line) or Trio-deficient (red line) embryos immunolabeled for phospho-MRLC. The means are calculated from ≥17 cells from at least four different lens pits. Statistical significant differences were evaluated by calculating *P*-values (see Materials and methods) for each pixel along the apical-basal axis. The blue line indicates the trend of statistical *P*-values subtracted from 1 and values greater than 0.95 ($P<0.05$) indicate regions in which a statistically significant difference in signal intensity is found. (**F**) The average cell shape for control and Trio-deficient lens pit cells was quantified. The numerical values above and below each shape indicate the fold difference compared with the average basal width of control cells.

DISCUSSION

RhoA/Rho-kinase signaling is required for Shroom3-dependent lens pit invagination

Previous work has indicated that the interaction between Shroom3 and Rock1/2 facilitates morphogenesis of the neural tube (Nishimura and Takeichi, 2008). Although we have previously shown that Shroom3 is required for AC during lens pit invagination (Plageman et al., 2010), it was unclear whether the function of Shroom3 was Rho-kinase dependent. In Y27632-treated embryos, lens pit invagination did not occur and AC was inhibited, an outcome that has been confirmed by others (Borges et al., 2011). Because Shroom3 mutants and Y27632-treated embryos both have a reduction in AC, it is reasonable to suggest that they function together during lens pit invagination. The disparity of phenotypic severity between the two experiments could be due to functional redundancy. Shroom3-related proteins, such as Shroom2, which plays a role in eye development and regulates Rock1/2-dependent contractility (Fairbank et al., 2006; Farber et al., 2011), might also preclude a more severe eye phenotype. The phenotypic severity was not due to a general failure of eye development as several lens differentiation markers were expressed in the uninvaginated placodal structure found in Y27632-treated embryos.

The data presented here demonstrate that Rock1/2 activity is essential for lens morphogenesis; however, the severity of the phenotype leaves open the possibility that morphogenesis of the lens might be secondarily affected. Unlike the Shroom3 mutants, lens pit invagination in Y7632-treated embryos failed altogether, the optic vesicle did not invaginate and morphogenesis of the entire eye was disrupted. Shroom3 mutants do have an optic vesicle phenotype (T.F.P. and R.A.L., unpublished) but, like in the lens, the phenotypic severity was not as great as Y27632-treated embryos. This discrepancy could be attributed to the wider range of tissues and cellular processes likely to be affected by Rho-kinase inhibition versus Shroom3 deletion. Similar to our data, optic-cup invagination also fails in Y27632-treated 3D embryonic stem cell aggregates that undergo morphogenesis spontaneously in culture (Eiraku et al., 2011). In addition to AC, invagination of the lens is likely to be facilitated through a close association with the underlying optic cup mediated by filipodia and extracellular matrix (Chauhan et al., 2009; Huang et al., 2011). When Rho-kinase function is inhibited, lens invagination failure could be due to combined disruption of lens placode AC and optic cup formation. Additionally, Rho-kinase has been implicated in processes other than AC, such as cytokinesis, apoptosis and migration (Riento and Ridley, 2003). It is possible that the severe phenotype was the result of a number of failed processes that normally contribute to morphogenesis.

The dependence of Shroom3-induced apical constriction on Rho-kinase activity suggested that RhoA, a major activator of Rock1/2, might also be required. However, it was previously shown that in the *Xenopus* blastula Shroom3-induced AC was not adversely affected when co-expressed with dominant-negative RhoA ($RhoA^{N19}$). This result was somewhat surprising considering the fact that dominant-negative Rho1, the *Drosophila* homolog of RhoA, inhibits AC and/or invagination in the wing disc, the salivary gland and the ventral furrow during gastrulation (Barrett et al., 1997; Xu et al., 2008; Zimmerman et al., 2010). Similarly, we observed that Shroom3-induced AC in MDCK cells was attenuated when $RhoA^{N19}$ was expressed or when treated with the RhoA chemical inhibitor G04. Furthermore, we observed that constitutively active RhoA and

the SD2 domain of Shroom3 simultaneously bind Rock1 in a complex, consistent with the idea that this interaction occurs during AC. In contrast to the data presented here, it was previously reported that RhoA^{N19} did not inhibit Shroom3-induced AC in MDCK cells (Hildebrand, 2005). In this experiment, Shroom3 was uniformly expressed in an inducible cell line rather than transiently in individual cells as performed here. These discrepancies could be due to the different cell types utilized in each experiment (MDCK cells versus *Xenopus* epithelia), differences in Shroom3 or RhoA^{N19} expression level ratios, or the effect of surrounding cells uniformly expressing Shroom3. We conclude that Shroom3-induced AC is dependent on RhoA in most contexts.

Apical localization of RhoA and Shroom3

In epithelial cells undergoing AC, active RhoA is localized apically (Simoes et al., 2006; Kinoshita et al., 2008). However, it has not been clear whether this localization was sufficient for AC. The data presented here show that AC is not induced upon expression of untargeted RhoA^{L63} in MDCK cells but is when RhoA^{L63} is apically localized. Similarly, basolaterally targeted RhoA^{L63} causes basal constriction, suggesting that localizing RhoA activity is a crucial step to shape epithelial cells during morphogenesis. In addition to inducing basal constriction, BL-RhoA^{L63} also appeared to at least partially reverse polarity and cause ZO1 to basally localize in structures that resembled tight-junctions. RhoA is known to regulate tight-junction formation and it was recently demonstrated that RhoA activity is locally activated to promote this process (Etienne-Manneville and Hall, 2002; Terry et al., 2011). Together, these data indicate that RhoA localization is important to properly elicit specific cellular processes such as AC.

It is hypothesized that the regulation of Shroom3 apical localization is a key step for AC. We have found that when RhoA is conditionally deleted in the lens pit, Shroom3 fails to apically localize and AC is reduced (Chauhan et al., 2011). These data are consistent with the idea that RhoA influences AC in part through the apical recruitment of Shroom3. Apical recruitment of the *Drosophila* homolog of Shroom3 depends on specific domains in the N-terminus, which are isoform-specific (Bolinger et al., 2010). This suggests that the mechanism by which RhoA directs Shroom3 localization involves the N-terminus. Cells expressing BL-RhoA^{L63} not only basally constrict but also basally recruit Shroom3, demonstrating that can RhoA direct the constriction machinery at either end of the cell. Although AC is known to modulate bending of several epithelia, the contribution of basal constriction has been less studied (Martinez-Morales et al., 2009). It will be interesting to determine whether RhoA and/or Shroom3 can direct basal constriction during morphogenesis.

The RhoA-GEF Trio activates RhoA/Shroom3-dependent apical constriction

One focus of this work was to determine what activates RhoA during Shroom3-induced AC. As Shroom3 does not contain the classic GEF DH/PH domains responsible for Rho-GTPase stimulation, we speculated that a RhoA-GEF was also required for AC. Although in vitro we found that Trio alone was not sufficient to induce AC, Trio inhibition in vivo, via transgenic expression of Tripα, prevents AC in the chick lens pit during invagination. Although Tripα can inhibit Shroom3-induced AC, Trio depletion by shRNA did not, perhaps suggesting that Tripα might affect an additional GEF. Of the several additional RhoA GEFs tested, only Kalirin showed any sensitivity to Tripα (Schmidt et al., 2002) and because Trio and Kalirin are homologous and co-expressed in MDCK cells and the lens pit, it is possible that they play overlapping roles during AC. This is further supported by the data demonstrating that in MDCK cells deficient for Trio and Kalirin, Shroom3-induced AC is inhibited. Given that the AC phenotype is greater in the Shroom3 mutants than in the Trio mutants it would be interesting to determine whether the AC phenotype is exacerbated in Trio-Kalirin double mutants.

The data presented here supports the hypothesis that Trio is a crucial activator of RhoA/Shroom3-dependent AC during invagination. When wild-type RhoA is apically localized in MDCK cells, AC is not induced; however, AC does occur when

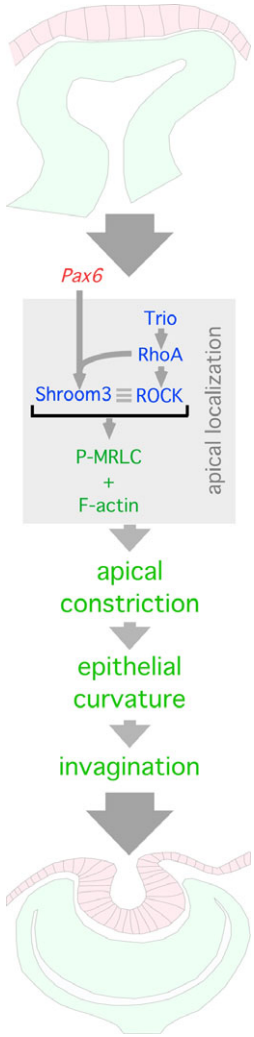

Fig. 7. A Trio-RhoA-Shroom3 pathway is required for apical constriction during lens pit invagination. Model depicting the proposed molecular pathway by which lens pit cell apical constriction drives invagination. Pax6 and RhoA regulate Shroom3 expression and apical localization, respectively. The Shroom3-dependent apical constriction machinery requires Trio activation of RhoA. This leads to activation of the contractile, actin-myosin network and a reduced apical circumference of cells. The coordinated action of a localized group of cells that are apically constricting causes inward bending and invagination of the epithelial placode forming the lens pit.

co-expressed with Trio. We also observed that mutation of the RhoA-specific GEF domain of Trio inhibits its contribution to Shroom3-induced AC. Importantly, Trio mutant mice also have a reduction in AC and activated myosin, which are phenotypes that bear a strong resemblance to RhoA and Shroom3 mutants (Chauhan et al., 2011). Together, these data are consistent with a model for AC in which an apically localized complex consisting of Trio, RhoA, Shroom3 and Rock1/2 function to activate the contractile actin-myosin network (Fig. 7). Although it is currently unknown whether Trio binds to Shroom3, we did observe that the SD2 domain of Shroom3, Rock1 and RhoA can interact simultaneously, supporting this model. It is likely that the pathway described here will function in many developmental events in which epithelia bend.

Acknowledgements
We thank Paul Speeg for excellent technical assistance and Dr Linda Levin of the Center for Clinical and Translational Science and Training at the University of Cincinnati for her help with statistical analysis.

Funding
We acknowledge grant support from the National Institutes of Health [R01 EY17848] and from the Abrahamson Pediatric Eye Institute Endowment at Children's Hospital Medical Center of Cincinnati to R.A.L.; the Agence Nationale de la Recherche [ANR-07-NEURO-006-01-BRAINGEF to A.D.]; the National Institutes of Health [R01 CA125658 to Y.Z.]; and the National Institute of General Medical Sciences [067525 to J.D.H.]. Deposited in PMC for release after 12 months.

Competing interests statement
The authors declare no competing financial interests.

References

Akaike, H. (1974). A new look at the statistical model identification. *IEEE Trans. Automat. Contr.* **19**, 716-723.
Alam, M. R., Johnson, R. C., Darlington, D. N., Hand, T. A., Mains, R. E. and Eipper, B. A. (1997). Kalirin, a cytosolic protein with spectrin-like and GDP/GTP exchange factor-like domains that interacts with peptidylglycine alpha-amidating monooxygenase, an integral membrane peptide-processing enzyme. *J. Biol. Chem.* **272**, 12667-12675.
Amano, M., Ito, M., Kimura, K., Fukata, Y., Chihara, K., Nakano, T., Matsuura, Y. and Kaibuchi, K. (1996). Phosphorylation and activation of myosin by Rho-associated kinase (Rho-kinase). *J. Biol. Chem.* **271**, 20246-20249.
Ashery-Padan, R., Marquardt, T., Zhou, X. and Gruss, P. (2000). Pax6 activity in the lens primordium is required for lens formation and for correct placement of a single retina in the eye. *Genes Dev.* **14**, 2701-2711.
Backer, S., Hidalgo-Sanchez, M., Offner, N., Portales-Casamar, E., Debant, A., Fort, P., Gauthier-Rouviere, C. and Bloch-Gallego, E. (2007). Trio controls the mature organization of neuronal clusters in the hindbrain. *J. Neurosci.* **27**, 10323-10332.
Barrett, K., Leptin, M. and Settleman, J. (1997). The Rho GTPase and a putative RhoGEF mediate a signaling pathway for the cell shape changes in Drosophila gastrulation. *Cell* **91**, 905-915.
Bellanger, J. M., Estrach, S., Schmidt, S., Briancon-Marjollet, A., Zugasti, O., Fromont, S. and Debant, A. (2003). Different regulation of the Trio Dbl-Homology domains by their associated PH domains. *Biol. Cell* **95**, 625-634.
Bolinger, C., Zasadil, L., Rizaldy, R. and Hildebrand, J. D. (2010). Specific isoforms of drosophila shroom define spatial requirements for the induction of apical constriction. *Dev. Dyn.* **239**, 2078-2093.
Borges, R. M., Lamers, M. L., Forti, F. L., Santos, M. F. and Yan, C. Y. (2011). Rho signaling pathway and apical constriction in the early lens placode. *Genesis* **49**, 368-379.
Briancon-Marjollet, A., Ghogha, A., Nawabi, H., Triki, I., Auziol, C., Fromont, S., Piche, C., Enslen, H., Chebli, K., Cloutier, J. F. et al. (2008). Trio mediates netrin-1-induced Rac1 activation in axon outgrowth and guidance. *Mol. Cell. Biol.* **28**, 2314-2323.
Charrasse, S., Comunale, F., Fortier, M., Portales-Casamar, E., Debant, A. and Gauthier-Rouviere, C. (2007). M-cadherin activates Rac1 GTPase through the Rho-GEF trio during myoblast fusion. *Mol. Biol. Cell* **18**, 1734-1743.
Chauhan, B. K., Disanza, A., Choi, S. Y., Faber, S. C., Lou, M., Beggs, H. E., Scita, G., Zheng, Y. and Lang, R. A. (2009). Cdc42- and IRSp53-dependent contractile filopodia tether presumptive lens and retina to coordinate epithelial invagination. *Development* **136**, 3657-3667.
Chauhan, B. K., Lou, M., Zheng, Y. and Lang, R. A. (2011). Balanced Rac1 and RhoA activities regulate cell shape and drive invagination morphogenesis in epithelia. *Proc. Natl. Acad. Sci. USA* (in press).
Debant, A., Serra-Pages, C., Seipel, K. O., Brien, S., Tang, M., Park, S. H. and Streuli, M. (1996). The multidomain protein Trio binds the LAR transmembrane tyrosine phosphatase, contains a protein kinase domain, and has separate rac-specific and rho-specific guanine nucleotide exchange factor domains. *Proc. Natl. Acad. Sci. USA* **93**, 5466-5471.
Eiraku, M., Takata, N., Ishibashi, H., Kawada, M., Sakakura, E., Okuda, S., Sekiguchi, K., Adachi, T. and Sasai, Y. (2011). Self-organizing optic-cup morphogenesis in three-dimensional culture. *Nature* **472**, 51-56.
Estrach, S., Schmidt, S., Diriong, S., Penna, A., Blangy, A., Fort, P. and Debant, A. (2002). The Human Rho-GEF trio and its target GTPase RhoG are involved in the NGF pathway, leading to neurite outgrowth. *Curr. Biol.* **12**, 307-312.
Etienne-Manneville, S. and Hall, A. (2002). Rho GTPases in cell biology. *Nature* **420**, 629-635.
Fairbank, P. D., Lee, C., Ellis, A., Hildebrand, J. D., Gross, J. M. and Wallingford, J. B. (2006). Shroom2 (APXL) regulates melanosome biogenesis and localization in the retinal pigment epithelium. *Development* **133**, 4109-4118.
Farber, M. J., Rizaldy, R. and Hildebrand, J. D. (2011). Shroom2 regulates contractility to control endothelial morphogenesis. *Mol. Biol. Cell* **22**, 795-805.
Fujisawa, K., Fujita, A., Ishizaki, T., Saito, Y. and Narumiya, S. (1996). Identification of the Rho-binding domain of p160ROCK, a Rho-associated coiled-coil containing protein kinase. *J. Biol. Chem.* **271**, 23022-23028.
Fukata, M., Nakagawa, M. and Kaibuchi, K. (2003). Roles of Rho-family GTPases in cell polarisation and directional migration. *Curr. Opin. Cell Biol.* **15**, 590-597.
Haigo, S. L., Hildebrand, J. D., Harland, R. M. and Wallingford, J. B. (2003). Shroom induces apical constriction and is required for hingepoint formation during neural tube closure. *Curr. Biol.* **13**, 2125-2137.
Hendrix, R. W. and Zwaan, J. (1974). Cell shape regulation and cell cycle in embryonic lens cells. *Nature* **247**, 145-147.
Hildebrand, J. D. (2005). Shroom regulates epithelial cell shape via the apical positioning of an actomyosin network. *J. Cell Sci.* **118**, 5191-5203.
Hildebrand, J. D. and Soriano, P. (1999). Shroom, a PDZ domain-containing actin-binding protein, is required for neural tube morphogenesis in mice. *Cell* **99**, 485-497.
Huang, J., Rajagopal, R., Liu, Y., Dattilo, L. K., Shaham, O., Ashery-Padan, R. and Beebe, D. C. (2011). The mechanism of lens placode formation: a case of matrix-mediated morphogenesis. *Dev. Biol.* **355**, 32-42.
Jaffe, A. B. and Hall, A. (2005). Rho GTPases: biochemistry and biology. *Annu. Rev. Cell Dev. Biol.* **21**, 247-269.
Kimura, K., Ito, M., Amano, M., Chihara, K., Fukata, Y., Nakafuku, M., Yamamori, B., Feng, J., Nakano, T., Okawa, K. et al. (1996). Regulation of myosin phosphatase by Rho and Rho-associated kinase (Rho-kinase). *Science* **273**, 245-248.
Kinoshita, N., Sasai, N., Misaki, K. and Yonemura, S. (2008). Apical accumulation of Rho in the neural plate is important for neural plate cell shape change and neural tube formation. *Mol. Biol. Cell* **19**, 2289-2299.
Lecuit, T. and Lenne, P. F. (2007). Cell surface mechanics and the control of cell shape, tissue patterns and morphogenesis. *Nat. Rev. Mol. Cell Biol.* **8**, 633-644.
Lee, C., Scherr, H. M. and Wallingford, J. B. (2007). Shroom family proteins regulate gamma-tubulin distribution and microtubule architecture during epithelial cell shape change. *Development* **134**, 1431-1441.
Martinez-Morales, J. R., Rembold, M., Greger, K., Simpson, J. C., Brown, K. E., Quiring, R., Pepperkok, R., Martin-Bermudo, M. D., Himmelbauer, H. and Wittbrodt, J. (2009). ojoplano-mediated basal constriction is essential for optic cup morphogenesis. *Development* **136**, 2165-2175.
Newsome, T. P., Schmidt, S., Dietzl, G., Keleman, K., Asling, B., Debant, A. and Dickson, B. J. (2000). Trio combines with dock to regulate Pak activity during photoreceptor axon pathfinding in *Drosophila*. *Cell* **101**, 283-294.
Nishimura, T. and Takeichi, M. (2008). Shroom3-mediated recruitment of Rho kinases to the apical cell junctions regulates epithelial and neuroepithelial planar remodeling. *Development* **135**, 1493-1502.
O'Brien, S. P., Seipel, K., Medley, Q. G., Bronson, R., Segal, R. and Streuli, M. (2000). Skeletal muscle deformity and neuronal disorder in Trio exchange factor-deficient mouse embryos. *Proc. Natl. Acad. Sci. USA* **97**, 12074-12078.
O'Keefe, L., Somers, W. G., Harley, A. and Saint, R. (2001). The pebble GTP exchange factor and the control of cytokinesis. *Cell Struct. Funct.* **26**, 619-626.
Peng, Y. J., He, W. Q., Tang, J., Tao, T., Chen, C., Gao, Y. Q., Zhang, W. C., He, X. Y., Dai, Y. Y., Zhu, N. C. et al. (2010). Trio is a key guanine nucleotide exchange factor coordinating regulation of the migration and morphogenesis of granule cells in the developing cerebellum. *J. Biol. Chem.* **285**, 24834-24844.
Plageman, T. F., Jr, Chung, M. I., Lou, M., Smith, A. N., Hildebrand, J. D., Wallingford, J. B. and Lang, R. A. (2010). Pax6-dependent Shroom3 expression regulates apical constriction during lens placode invagination. *Development* **137**, 405-415.

Riento, K. and Ridley, A. J. (2003). Rocks: multifunctional kinases in cell behaviour. *Nat. Rev. Mol. Cell Biol.* **4**, 446-456.
Sawyer, J. M., Harrell, J. R., Shemer, G., Sullivan-Brown, J., Roh-Johnson, M. and Goldstein, B. (2010). Apical constriction: a cell shape change that can drive morphogenesis. *Dev. Biol.* **341**, 5-19.
Schmidt, S., Diriong, S., Mery, J., Fabbrizio, E. and Debant, A. (2002). Identification of the first Rho-GEF inhibitor, TRIPalpha, which targets the RhoA-specific GEF domain of Trio. *FEBS Lett.* **523**, 35-42.
Simoes, S., Denholm, B., Azevedo, D., Sotillos, S., Martin, P., Skaer, H., Hombria, J. C. and Jacinto, A. (2006). Compartmentalisation of Rho regulators directs cell invagination during tissue morphogenesis. *Development* **133**, 4257-4267.
Smallhorn, M., Murray, M. J. and Saint, R. (2004). The epithelial-mesenchymal transition of the *Drosophila* mesoderm requires the Rho GTP exchange factor Pebble. *Development* **131**, 2641-2651.
Smith, A. N., Miller, L. A., Song, N., Taketo, M. M. and Lang, R. A. (2005). The duality of beta-catenin function: a requirement in lens morphogenesis and signaling suppression of lens fate in periocular ectoderm. *Dev. Biol.* **285**, 477-489.
Smith, A. N., Miller, L. A., Radice, G., Ashery-Padan, R. and Lang, R. A. (2009). Stage-dependent modes of Pax6-Sox2 epistasis regulate lens development and eye morphogenesis. *Development* **136**, 2977-2985.
Stewart, S. A., Dykxhoorn, D. M., Palliser, D., Mizuno, H., Yu, E. Y., An, D. S., Sabatini, D. M., Chen, I. S., Hahn, W. C., Sharp, P. A. et al. (2003). Lentivirus-delivered stable gene silencing by RNAi in primary cells. *RNA* **9**, 493-501.
Terry, S. J., Zihni, C., Elbediwy, A., Vitiello, E., Leefa Chong, San, I. V., Balda, M. S. and Matter, K. (2011). Spatially restricted activation of RhoA signalling at epithelial junctions by p114RhoGEF drives junction formation and morphogenesis. *Nat. Cell Biol.* **13**, 159-166.
Toresson, H., Mata de Urquiza, A., Fagerstrom, C., Perlmann, T. and Campbell, K. (1999). Retinoids are produced by glia in the lateral ganglionic eminence and regulate striatal neuron differentiation. *Development* **126**, 1317-1326.
Totsukawa, G., Yamakita, Y., Yamashiro, S., Hartshorne, D. J., Sasaki, Y. and Matsumura, F. (2000). Distinct roles of ROCK (Rho-kinase) and MLCK in spatial regulation of MLC phosphorylation for assembly of stress fibers and focal adhesions in 3T3 fibroblasts. *J. Cell Biol.* **150**, 797-806.
van Impel, A., Schumacher, S., Draga, M., Herz, H. M., Grosshans, J. and Muller, H. A. (2009). Regulation of the Rac GTPase pathway by the multifunctional Rho GEF Pebble is essential for mesoderm migration in the *Drosophila* gastrula. *Development* **136**, 813-822.
Wei, L., Roberts, W., Wang, L., Yamada, M., Zhang, S., Zhao, Z., Rivkees, S. A., Schwartz, R. J. and Imanaka-Yoshida, K. (2001). Rho kinases play an obligatory role in vertebrate embryonic organogenesis. *Development* **128**, 2953-2962.
Xu, N., Keung, B. and Myat, M. M. (2008). Rho GTPase controls invagination and cohesive migration of the *Drosophila* salivary gland through Crumbs and Rho-kinase. *Dev. Biol.* **321**, 88-100.
Zimmerman, S. G., Thorpe, L. M., Medrano, V. R., Mallozzi, C. A. and McCartney, B. M. (2010). Apical constriction and invagination downstream of the canonical Wnt signaling pathway require Rho1 and Myosin II. *Dev. Biol.* **340**, 54-66.